

Wave height distributions on shallow foreshores

Jurjen A. Battjes^{a,*}, Heiko W. Groenendijk¹

^a *Department of Civil Engineering, Delft University of Technology, P.O. Box 5048,
2600 GA Delft, Netherlands*

Received 24 March 1999; received in revised form 7 January 2000; accepted 10 January 2000

Abstract

Wave height distributions on shallow foreshores deviate from those in deep water due to the effects of the restricted depth-to-height ratio and of wave breaking. Laboratory data of wave heights on shallow foreshores of different slopes have been analysed to determine these effects and to derive generalised empirical parameterisations. A model distribution is proposed consisting of a Rayleigh distribution, or a Weibull distribution with exponent equal to 2, for the lower heights and a Weibull with a higher exponent for the higher wave heights. The parameters of this distribution have been estimated from the data and expressed in terms of local wave energy, depth and bottom slope, yielding a predictive model that is found to be significantly more accurate than existing expressions. © 2000 Elsevier Science B.V. All rights reserved.

1. Introduction

Wave characteristics in shallow water are frequently calculated from deep-water data with a wave energy model. Such models give the local wave energy (and, depending on the model chosen, its spectral distribution) but not wave height distributions, although these can play a role in design and evaluation of coastal structures.

In deep water, the approximately linear behaviour of the waves allows for a theoretically sound statistical description of the wave characteristics, based on a Gaussian distribution of instantaneous values of surface elevation, resulting in a Rayleigh distribution of (crest-to-trough) wave heights that is fully determined by the

* Corresponding author. Tel.: +31-152785060; fax: +31-152784842.

E-mail address: j.battjes@ct.tudelft.nl (J.A. Battjes).

¹ Former graduate student, Department of Civil Engineering, Delft University of Technology and formerly at WL/Delft Hydraulics, P.O. Box 177, 2600 MH Delft, The Netherlands.

local wave energy. In shallow water, the wave behaviour is more complicated and the knowledge of the statistical description of wave field characteristics is more limited. A situation of engineering significance occurs when waves propagate over a gently sloping shallow part of the coast seaward of a sea-defence work, a so-called shallow foreshore, where depth-induced breaking can cause the distribution of wave heights to differ considerably from the Rayleigh distribution, in a manner that at present is not well known.

Design criteria for coastal structures with respect to wave forces, cover layer stability, wave run-up or wave overtopping, involve one or another characteristic wave height of the incident waves, typically the significant wave height H_s (either $H_{1/3}$, the average of the highest 1/3 of the wave heights, or H_{m_0} , defined as $4/m_0$, four times the standard deviation of the surface elevation), or a wave height with some low exceedance probability (e.g. 1%, 0.1%, etc.). If the wave heights are Rayleigh-distributed, these heights can all be converted one into another through known constants, but if the distribution is distorted, e.g. due to shallow-water breaking as in the situations considered here, these ratios are not constants and not known.

The purpose of this paper is to present, analyse and parameterise laboratory data of wave height distributions on shallow foreshores. The parameterisation is based on the assumption of slow evolution, such that the distribution depends on local parameters only, regardless of the history of the waves in deeper water (a so-called point model). This assumption proves to be valid for shallow water with a reasonably simple bottom topography, although some slope dependence is apparent (see below). The parameterisation of the data utilises a combination of two Weibull distributions, calibrated and validated with laboratory data. The result is a predictive point model for the local wave height distribution, which uses as input only the local wave energy, depth and bottom slope, which are assumed to be known from given input data and from state-of-the-art shallow-water (spectral) wave energy models, respectively.

2. Existing models

2.1. Rayleigh wave height distribution

The short-term statistics of waves in deep water are well known (see Ochi, 1998 for a review). Based on the linear model of waves with a narrow energy spectrum, Longuet-Higgins (1952) showed that the heights of these waves obey the Rayleigh distribution, here written as

$$F_H \equiv \Pr\{\underline{H} < H\} = 1 - \exp\left[-\left(\frac{H}{H_{\text{rms}}}\right)^2\right] \quad (1)$$

in which H_{rms} is the root-mean-square (rms) wave height. Since the Rayleigh distribution has only one scale parameter and no shape parameter, fixed ratios exist between characteristic wave heights, i.e. $H_{1/3}/H_{\text{rms}} \approx 1.416$, $\mu_H/H_{\text{rms}} = 1/2\sqrt{\pi} \approx 0.886$ etc.,

where $H_{1/3}$ is the mean of the highest 1/3-part of the wave heights or the significant wave height and μ_H is the mean of all wave heights.

When a narrow frequency spectrum is assumed, all characteristic wave heights are theoretically proportional to the standard deviation of the water surface elevation with known proportionality constants, for example $H_{\text{rms}} = \sqrt{8m_0}$ and $H_{1/3} \approx 4\sqrt{m_0}$. For wind-driven sea waves, the assumption of a narrow-banded frequency spectrum is no longer valid. In deep water, the Rayleigh distribution as defined in Eq. (1) still holds to a very good approximation for the zero-crossing wave heights (Longuet-Higgins, 1980; Tayfun, 1990), but the ratios of wave height to standard deviation $\sqrt{m_0}$ have to be reduced to account for the finite frequency bandwidth. Goda (1979) analysed field data and found that for wind-driven waves in deep water, the ratio $H_{1/3}/\sqrt{m_0}$ is approximately 3.8 instead of the narrow-band value of 4.0, a reduction of 5%. The heights are still Rayleigh-distributed, so this means that for wind-driven waves in deep water, all ratios of wave height to $\sqrt{m_0}$ are 5% less than those given above, e.g. $H_{\text{rms}}/\sqrt{m_0} \approx 0.95 \times \sqrt{8} \approx 2.69 \approx 2.7$.

2.2. Distributions of depth-limited breaking wave heights

In shallow water, the situation changes considerably. Shoaling, triad interactions and depth-induced breaking become relevant. Shoaling enhances the triad interactions, which cause profile distortion (bound spectral components) with an excess of crest height and shallow troughs, in contrast to the Gaussian waves in deep water. Thus, the surface elevation in shallow water can no longer be considered a narrow-banded linear Gaussian process. This poses a problem for the description of wave statistics in shallow water. Wave breaking only aggravates this situation. Two approaches have been advanced to deal with this situation.

Collins (1970), Mase and Iwagaki (1982) and Dally and Dean (1986) have presented a method for the calculation of the distribution of the heights of waves breaking in shallow water. Given a sequence of wave heights and periods (between zero up-or down-crossings) and directions at some offshore location, or a joint probability distribution of those variables, they apply a monochromatic wave model for shoaling and breaking to each class of them to calculate the onshore transformation of that monochromatic wave class. Combining the results at any given inshore location, taking the probability of each class at the offshore location into account, allows the construction of the local, inshore wave height distribution. Dally (1990, 1992) and Kuriyama (1996) have elaborated on this approach. These methods are algorithmic and do not result in explicit expressions for further analyses or extrapolation to low probabilities of exceedance.

Another approach, which is also pursued in this paper, consists of making (semi)-empirical adaptations to the Rayleigh distribution of the wave heights to allow for the effects of shallow water and breaking, resulting in explicit analytical expressions suitable for further mathematical manipulations. Glukhovskiy (1966) proposed a distribution that takes the influence of depth-limited breaking into account by making the exponent in the right-hand side of Eq. (1) an increasing function of the wave height-to-

depth ratio, thus modifying the shape of the distribution. We present here only the modified Glukhovskiy distribution as given by Klopman (1996):

$$F_{\underline{H}}(H) \equiv \Pr\{\underline{H} \leq H\} = 1 - \exp\left(-A \left(\frac{H}{H_{\text{rms}}}\right)^\kappa\right) \quad (2)$$

To assure consistency, the second moment of the modified Glukhovskiy probability density function has to equal $(H_{\text{rms}})^2$. This yields the following relation between the coefficient A and the exponent κ :

$$A = \left[\Gamma\left(\frac{2}{\kappa} + 1\right) \right]^{\frac{\kappa}{2}} \quad (3)$$

The exponent κ is assumed to be a function of the ratio of rms wave height to water depth, $H^* \equiv H_{\text{rms}}/d$:

$$\kappa = \frac{2}{1 - \beta H^*} \quad (4)$$

For sufficiently low wave height-to-water depth ratio, $H^* \rightarrow 0$ and $\kappa \rightarrow 2$, in which case the Rayleigh distribution is recovered.

Klopman assumes the relation between H_{rms} and m_0 to be as for a narrow-banded Gaussian process: $H_{\text{rms}} = \sqrt{(8m_0)}$. Eq. (4) has been fitted to laboratory data, yielding $\beta = 0.7$ as the optimal value (Klopman, 1996).

Just as the Rayleigh distribution, the Glukhovskiy distribution is actually a special case of the more general Weibull distribution, which allows for an arbitrary exponent in the expression for the exceedance probability (right-hand side in Eq. (1)).

Tayfun (1981) has presented a theoretical model for the distribution of wave heights, including the effect of wave breaking, based on a narrow-band random phase model with a finite number of spectral components (N) such that there is a maximum obtainable wave height, with a value estimated on the basis of the expression of Miche (1944) for the highest periodic wave of permanent form. However, the expression in Tayfun (1981) for the maximum possible normalised amplitude in terms of N is too large by a factor $\sqrt{2}$, as acknowledged by Tayfun (1999), which also renders the expressions for the probability distribution of the normalised wave heights invalid. Moreover, for waves breaking in shallow water, as occurs in many of the data to be used below, the required value of N becomes so low that the theoretical probability of the wave heights takes on an unrealistic, jagged appearance. For these reasons, this theoretical distribution is not included in the model-data comparison to be given below.

The distributions given by Glukhovskiy and by Tayfun are both point models, yielding a local wave height distribution for given local depth d and wave parameters (lowest two spectral moments).

2.3. Evaluation of existing models

To give some insight in the performance of existing analytical models on a shallow foreshore, Fig. 1 shows a typical empirical cumulative distribution of wave heights,

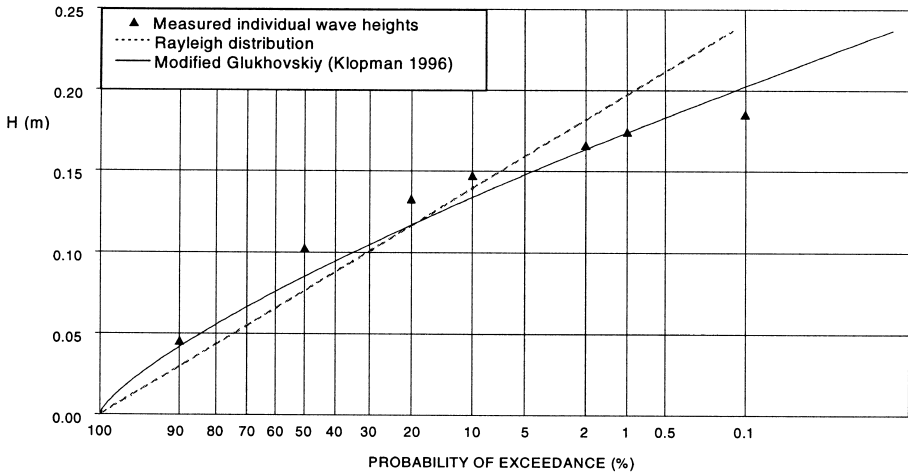


Fig. 1. Example of calculated wave height distributions; slope 1:100, $H_{m_0} = 0.13$ m and $d = 0.27$ m.

measured in a wave flume over a plane shallow foreshore with a slope of 1:100 (Van der Meer, 1988) at a location where the measured water surface elevation variance equals $m_0 = 1.1E - 3$ m² and the water depth $d = 0.27$ m (thus, $H_{m_0} \approx 0.13$ m $\approx 0.5 d$). The straight, dotted line is the Rayleigh distribution and the solid line represents the modified Glukhovskiy distribution, both with $H_{rms} = \sqrt{(8m_0)}$.

Fig. 1 shows that the Rayleigh distribution, with $H_{rms} = \sqrt{(8m_0)}$, gives a poor description of the measured wave height distribution. In particular, it significantly underestimates the lower wave heights and overestimates the higher ones, for given probability of exceedance. The modified Glukhovskiy distribution, taking depth-induced breaking into account, yields a better approximation of the measured wave heights. However, in general, this distribution still overestimates the extreme wave heights and underestimates the lower wave heights on shallow foreshores. That is why a better description of the observed data is sought.

3. Composite Weibull wave height distribution

3.1. Definition

Inspection of numerous empirical wave height distributions on shallow foreshores, plotted on Rayleigh paper, showed a marked transition between a linear trend for the lower heights and a downward curved relation for the higher waves. Such abrupt transition does not lend itself to a distribution with a single expression and one shape parameter. Therefore, as a working hypothesis, a combination of two Weibull distributions was assumed, each having a different exponent, matched at the transition wave

height H_{tr} , the so-called Composite Weibull distribution (to be referred to as CWD hereafter):

$$F(H) \equiv \Pr\{\underline{H} \leq H\} = \begin{cases} F_1(H) = 1 - \exp\left[-\left(\frac{H}{H_1}\right)^{k_1}\right] & H \leq H_{tr} \\ F_2(H) = 1 - \exp\left[-\left(\frac{H}{H_2}\right)^{k_2}\right] & H \geq H_{tr} \end{cases} \quad (5)$$

In order to obtain continuity of the distribution function, the constraint $F_1(H_{tr}) = F_2(H_{tr})$ is imposed. The exponents k_1 and k_2 are shape parameters of the distribution. They determine the curvature of the corresponding part of the distribution. H_1 and H_2 are scale parameters.

Because the values of k_1 and k_2 do not match at the transition point, the probability density is discontinuous there. This is physically not realistic but it is nevertheless accepted because all integral statistical properties of the wave heights are well behaved.

In the following section, we present data sets that have been used to calibrate and validate the assumed model distribution.

4. Data

In order to relate the independent parameters of the CWD to a certain wave field, measured wave height distributions, corresponding local water depths and spectral moments are required for different foreshore slopes. These were obtained from experiments performed by WL/Delft hydraulics in the context of other studies in a 50-m long, 1.0-m wide and 1.2-m deep wave flume equipped with a wave maker capable of generating random waves and absorbing incoming wave energy. At the back of the wave

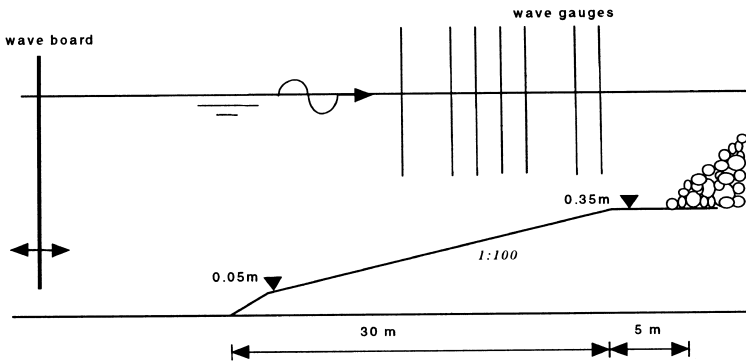


Fig. 2. Shallow foreshore test set-up; slope 1:100.

Table 1

Available shallow foreshore data

Sixth column: ratio of local significant wave height to the value at deep water. Eighth column: deep water steepness based on significant wave height and spectral peak frequency. Note: for the 1:20 and 1:50 slopes, the data were used both for calibration and validation; no data for the 1:30 slope were used in the calibration, whereas for the 1:100 as well as for the 1:250 slope, two non-overlapping sets of data were used, one for calibration and another one for validation

Slope	Project author	Number of tests	Number of gauges	Range of $H_{1/3}/d$	Range of $H_{1/3}/H_{1/3,0}$	Range of $\psi = \sqrt{m_0}/d$	Range of S_{op}	Number of waves
1:20	H1874 (Gerding, 1993)	22	4	0.3–0.83	1.1–0.75	0.044–0.137	0.01–0.04	1000
1:30	H3356 (Bhageloe, 1998)	21	7	0.1–0.6	1.1–0.8	0.025–0.15	0.015–0.05	500
1:50	H1874/50 (Gerding, 1993)	16	4	0.2–0.65	1.1–0.72	0.035–0.154	0.017–0.04	200
1:100	H1256 (Van der Meer, 1993)	17	18	0.13–0.6	1.1–0.51	0.04–0.16	0.01–0.04	1100
1:250	H0462.25 (Van der Meer, 1988)	72	19	0.3–0.6	1.15–0.35	0.03–0.15	0.008–0.03	1000

flume, a spending beach provides passive wave damping. An overview of a typical test set-up for a shallow foreshore is given in Fig. 2.

Tests have been performed for shallow foreshores with slopes 1:20, 1:30, 1:50, 1:100 and 1:250. Table 1 gives an overview including references (see Groenendijk and Van Gent (1998) for more details). During a test, a number of waves was generated by the wave maker, with a standard JONSWAP spectrum ($\gamma = 3.3$) as a target. Wave gauges were placed along the shallow foreshore to measure the surface elevation at locations of different still water depths, d . From the measured surface elevations, statistical measures of wave height like H_{rms} , $H_{1\%}$ etc., wave height distributions and spectral moments have been determined. (The filed spectral moments, used below, include contributions from the low-frequency waves; the raw data were not available for filtering these out.)

From the available data, two sets were selected, one set for calibration and another, partially overlapping set for validation (see Table 1).

5. Calibration and parameterisation of model parameters

5.1. Approach

In all, the CWD as formulated in Eq. (5) has five parameters, of which four are independent because of the imposed continuity of $F(H)$ at H_{tr} . These will be estimated from the records of the data set for calibration and subsequently be parameterised in terms of controlling external variables like wave energy and water depth.

The scale parameters H_1 and H_2 are convenient in the formulation in Eq. (5), but they have no direct clear physical meaning. Therefore, one of them is abandoned as an independent parameter, which is possible in view of the continuity constraint, and the other is replaced in the set of independent parameters by the rms value of all the wave heights (H_{rms}), leaving the independent set of parameters k_1 , k_2 , H_{tr} and H_{rms} as the unknowns to be estimated and parameterised. Together with the continuity constraint, they determine H_1 and H_2 and so the entire distribution as formulated in Eq. (5).

In the following, we first make estimates of the exponents k_1 and k_2 . Once these are known, only two independent parameters remain, H_{tr} and H_{rms} . By normalising all wave heights with H_{rms} , one of these is (temporarily) eliminated, leaving the location of the transition point as the only independent (shape) parameter of the distribution of the normalised wave heights. This allows us to consider the intrinsic properties of the wave height distribution, i.e. the relations among the wave heights as such.

Secondly, we determine relations between the parameters of the distribution and external parameters like the local depth, bottom slope and wave energy (spectrum). The ratio $\psi \equiv \sqrt{m_0}/d$ is a measure of the relative wave intensity, or degree of saturation. We use that as the most important independent normalised variable in the present context. (It may be more customary to use a wave height-to-depth ratio for this, such as H_s/d , but we want to avoid confusion or misunderstanding that can easily arise as a result of the varying definitions and, more importantly, unknown ratios between different characteristic wave heights, which is exactly the subject of the present paper.) The bottom slope is also taken into account but that is rather of a secondary nature.

Table 2

Characteristic normalised wave heights \tilde{H}_x as a function of \tilde{H}_r

\tilde{H}_r	\tilde{H}_1	\tilde{H}_2	$\tilde{H}_{1/3}$	$\tilde{H}_{1/10}$	$\tilde{H}_{2\%}$	$\tilde{H}_{1\%}$	$\tilde{H}_{0.1\%}$
0.05	12.193	1.060	1.279	1.466	1.548	1.620	1.813
0.1	7.003	1.060	1.279	1.466	1.548	1.620	1.813
0.15	5.063	1.060	1.279	1.466	1.548	1.620	1.813
0.2	4.022	1.060	1.279	1.466	1.548	1.620	1.813
0.25	3.365	1.060	1.279	1.466	1.548	1.620	1.813
0.3	2.908	1.060	1.279	1.466	1.548	1.620	1.813
0.35	2.571	1.060	1.279	1.466	1.548	1.620	1.813
0.4	2.311	1.060	1.279	1.466	1.548	1.620	1.813
0.45	2.104	1.060	1.279	1.466	1.549	1.620	1.813
0.5	1.936	1.061	1.280	1.467	1.549	1.621	1.814
0.55	1.796	1.061	1.281	1.468	1.550	1.622	1.815
0.6	1.678	1.062	1.282	1.469	1.552	1.624	1.817
0.65	1.578	1.064	1.284	1.471	1.554	1.626	1.820
0.7	1.492	1.066	1.286	1.474	1.557	1.629	1.823
0.75	1.419	1.069	1.290	1.478	1.561	1.634	1.828
0.8	1.356	1.073	1.294	1.483	1.567	1.639	1.835
0.85	1.302	1.077	1.300	1.490	1.573	1.646	1.843
0.9	1.256	1.083	1.307	1.498	1.582	1.655	1.852
0.95	1.216	1.090	1.315	1.507	1.591	1.665	1.864
1	1.182	1.097	1.324	1.518	1.603	1.677	1.877
1.05	1.153	1.106	1.335	1.530	1.616	1.690	1.892
1.1	1.128	1.116	1.346	1.543	1.630	1.705	1.909
1.15	1.108	1.126	1.359	1.558	1.645	1.721	1.927
1.2	1.090	1.138	1.371	1.573	1.662	1.739	1.946
1.25	1.075	1.150	1.381	1.590	1.679	1.757	1.967
1.3	1.063	1.162	1.389	1.607	1.698	1.776	1.988
1.35	1.052	1.175	1.395	1.626	1.717	1.796	2.011
1.4	1.043	1.189	1.399	1.644	1.737	1.817	2.034
1.45	1.036	1.203	1.403	1.664	1.757	1.838	2.058
1.5	1.030	1.217	1.406	1.683	1.778	1.860	2.082
1.55	1.024	1.231	1.408	1.703	1.799	1.882	2.106
1.6	1.020	1.246	1.410	1.721	1.820	1.904	2.131
1.65	1.016	1.261	1.411	1.736	1.841	1.927	2.156
1.7	1.013	1.275	1.412	1.749	1.863	1.949	2.182
1.75	1.011	1.290	1.413	1.759	1.884	1.972	2.207
1.8	1.009	1.305	1.413	1.767	1.906	1.994	2.232
1.85	1.007	1.320	1.414	1.773	1.927	2.017	2.257
1.9	1.006	1.334	1.414	1.779	1.949	2.039	2.282
1.95	1.004	1.349	1.415	1.783	1.970	2.062	2.307
2	1.004	1.363	1.415	1.786	1.985	2.084	2.332
2.05	1.003	1.378	1.415	1.789	1.983	2.106	2.357
2.1	1.002	1.392	1.415	1.791	1.982	2.128	2.382
2.15	1.002	1.407	1.415	1.793	1.981	2.150	2.406
2.2	1.001	1.421	1.415	1.795	1.981	2.149	2.430
2.25	1.001	1.435	1.415	1.796	1.980	2.148	2.454
2.3	1.001	1.449	1.415	1.797	1.979	2.148	2.478
2.35	1.001	1.462	1.415	1.797	1.979	2.147	2.502
2.4	1.000	1.476	1.416	1.798	1.979	2.147	2.525
2.45	1.000	1.490	1.416	1.798	1.979	2.147	2.548

Table 2 (continued)

\tilde{H}_{tr}	\tilde{H}_1	\tilde{H}_2	$\tilde{H}_{1/3}$	$\tilde{H}_{1/10}$	$\tilde{H}_{2\%}$	$\tilde{H}_{1\%}$	$\tilde{H}_{0.1\%}$
2.5	1.000	1.503	1.416	1.799	1.978	2.147	2.571
2.55	1.000	1.516	1.416	1.799	1.978	2.146	2.593
2.6	1.000	1.529	1.416	1.799	1.978	2.146	2.616
2.65	1.000	1.542	1.416	1.799	1.978	2.146	2.629
2.7	1.000	1.555	1.416	1.799	1.978	2.146	2.629
2.75	1.000	1.568	1.416	1.800	1.978	2.146	2.628
2.8	1.000	1.580	1.416	1.800	1.978	2.146	2.628
2.85	1.000	1.593	1.416	1.800	1.978	2.146	2.628
2.9	1.000	1.605	1.416	1.800	1.978	2.146	2.628
2.95	1.000	1.617	1.416	1.800	1.978	2.146	2.628
3	1.000	1.630	1.416	1.800	1.978	2.146	2.628

following and also shown in Fig. 3. With the values of k_1 and k_2 fixed, the CWD has only two independent parameters left.

5.3. Normalised wave height distribution

We normalise all wave heights with H_{rms} , to be indicated with a tilde:

$$\tilde{H}_x = \frac{H_x}{H_{rms}} \tag{6}$$

The mean square normalised wave height, or the second moment of the pdf of the CWD of the normalised wave heights, has to equal unity. This moment can be calculated from Eq. (5) in a straightforward manner, resulting in the following expression in terms of incomplete gamma functions $\gamma(a, x)$ and $\Gamma(a, x)$ (Abramowitz and Stegun, 1964, Eqs. 6.5.2. and 6.5.3):

$$\tilde{H}_{rms} = \sqrt{\tilde{H}_1^2 \gamma\left[\frac{2}{k_1} + 1, \left(\frac{\tilde{H}_{tr}}{\tilde{H}_1}\right)^{k_1}\right] + \tilde{H}_2^2 \Gamma\left[\frac{2}{k_2} + 1, \left(\frac{\tilde{H}_{tr}}{\tilde{H}_2}\right)^{k_2}\right]} = 1 \tag{7}$$

Because of this constraint, and in view of the fixed numerical values of the exponents k_1 and k_2 , the CWD of the normalised heights has only one independent (shape) parameter, the normalised transition height \tilde{H}_{tr} . This means that all conceivable normalised characteristic wave heights are a function of \tilde{H}_{tr} only. Analytical expressions for these values (ratios) can be derived in a straightforward manner, with the results expressed in terms of incomplete gamma functions similar to Eq. (7) (see Groenendijk, 1998 for details). Also, the wave height exceedance probability at the transition point is a function of \tilde{H}_{tr} only. Table 2 presents the results for the normalised values of the scale parameters H_1 and H_2 introduced in Eq. (5), $H_{1/3}$ and $H_{1/10}$, the average of the highest 1/3 and 1/10 of the wave heights, and the heights with probabilities of exceedance equal to 2%, 1% and 0.1%, as a function of \tilde{H}_{tr} . For $\tilde{H}_{tr} \rightarrow \infty$, the values approach those of the Rayleigh distribution. Convergence to this limit is reached to within four significant figures for values of \tilde{H}_{tr} greater than 2.75, as can be seen in Table 2.

It should be noted that the results above including those in Table 2 are independent of the actual values of H_{tr} and H_{rms} or their parameterisations, but for practical use, we need to know their values. This is addressed in the following.

5.4. Transitional wave height

In the philosophy of a point model, we relate H_{tr} and H_{rms} to the local depth, bottom slope and wave energy(spectrum).

At the transitional wave height, the wave height distribution abruptly changes its shape. This change in shape is ascribed to depth-induced breaking. Therefore, we assume that H_{tr} can be expressed as a kind of limiting wave height for nonbreaking waves. To do this, we first scale H_{tr} with d , as for purely depth-limited breaking. Thereafter, we consider the effect of wave steepness through a Miche-type breaker criterion.

5.4.1. Depth-limited transitional wave height

As mentioned above, values of the transitional wave height have been determined by least-squares fitting of the CWD to each of the wave height distributions in the data set selected for calibration, covering four different foreshore slopes. The estimated transitional wave heights, nondimensionalised with the water depth, are plotted as a function of the degree of saturation in Fig. 4. The ratio H_{tr}/d can be seen to be roughly independent of the degree of saturation (ψ) except for the relatively low waves (approximately $\psi < 0.06$), with some scatter that increases with increasing bottom slope. For simplicity, the scatter and the deviating behaviour for low relative heights are ignored and the transitional wave height is assumed to be proportional to the depth with a slope-dependent coefficient, $\gamma_{tr}(\alpha)$:

$$H_{tr} = \gamma_{tr}(\alpha) d \quad (8)$$

For each slope, a representative value of γ_{tr} is determined as the average of the estimated values of H_{tr}/d , represented by the solid lines in Fig. 4, based on only the values of H_{tr}/d for $\psi > 0.06$. Fig. 5 gives a plot of γ_{tr} so obtained versus the foreshore slope ($\tan \alpha$), showing that a steeper bottom slope leads to a higher γ_{tr} and therefore to a higher transitional wave height. This means that on a steeper slope, fewer waves deviate from the Rayleigh distribution than on a milder slope, other things being the same. This is consistent with a spatial lag in the process of breaking compared to depth changes.

Assuming a linear variation of γ_{tr} with the foreshore slope as in $\gamma_{tr} = c_1 + c_2 \tan \alpha$, we obtain $c_1 = 0.35$ and $c_2 = 5.8$ from the data in Fig. 5. With this slope-dependent γ_{tr} , local transitional wave heights in the CWD can be determined for given local depth and foreshore slope. (This parameterisation is part of the overall model and does not constitute a proposal for yet another breaker criterion to be used outside the present context.)

5.4.2. Depth- and steepness-limited transitional wave height

Fig. 4 shows that the assumption of a constant ratio of transitional wave height to water depth (for given slope) overestimates the nondimensional transitional wave height

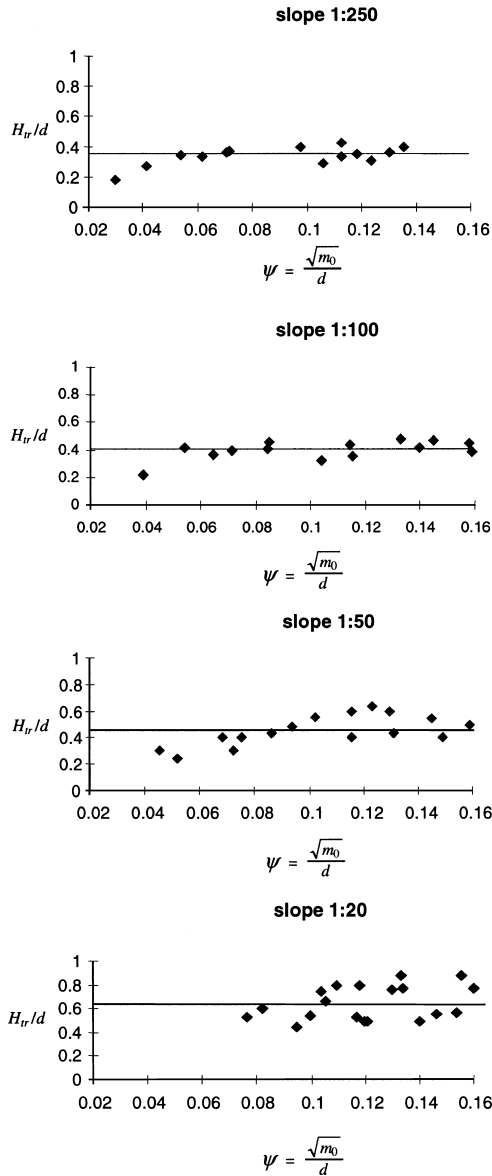


Fig. 4. Nondimensional transitional wave height versus the degree of saturation for different foreshore slopes.

for $\psi < 0.06$. The lower values of ψ represent relatively low waves compared to the depth. In those circumstances, the waves are more limited by the maximum wave steepness than by a limited water depth. By taking the wave steepness into account, a better approximation of the measured transitional wave height might be achieved.

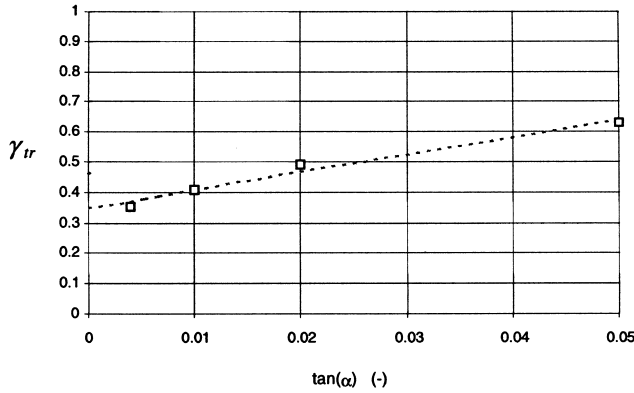


Fig. 5. Coefficient γ_{tr} versus foreshore slope.

Miche (1944) determined an approximate expression for the maximum height of a periodic wave of constant form in which limiting effects of both depth and steepness are included. Assuming that the transitional wave height behaves similar to Miche’s maximum wave height, we pose the following relation for H_{tr} :

$$H_{tr} = \beta_{tr} 0.14 L_c \tanh\left(\frac{2\pi d}{L_c}\right) \tag{9}$$

in which β_{tr} denotes a slope-dependent coefficient and L_c is a characteristic local wave length defined by

$$L_c = \frac{gT_c^2}{2\pi} \tanh\left(\frac{2\pi d}{L_c}\right) \tag{10}$$

in which T_c is a characteristic wave period. Here, the wave period $T_{0,2} = (m_0/m_2)^{1/2}$ is used for T_c (m_0 and m_2 are the local zero-th and second spectral moments). For each of the bottom slopes in the calibration data set, a single value of β_{tr} has been estimated using a least squares optimisation method. Fig. 6 shows the results. Assuming β_{tr} to be linearly dependent on the bottom slope as in $\beta_{tr} = c_3 + c_4 \tan \alpha$, we obtain $c_3 = 0.46$ and $c_4 = 9.25$, based on the data in Fig. 6. With this slope-dependent β_{tr} , the transitional wave height of the CWD can be determined for given depth, foreshore slope and wave period $T_{0,2}$.

Including a wave steepness effect in the estimation of the transitional wave height gives a slightly improved model performance in the end results (as will be shown), at the expense of an additional parameter, viz. a characteristic wave period. The choice of using $T_{0,2}$ in Eq. (10) is somewhat arbitrary. Whether another choice of characteristic period is more satisfactory has not been investigated, mainly for the reason that the effect of inclusion of period influence instead of the simpler Eq. (8) is rather weak anyway. In the end, we recommend not to use the steepness dependence at all.

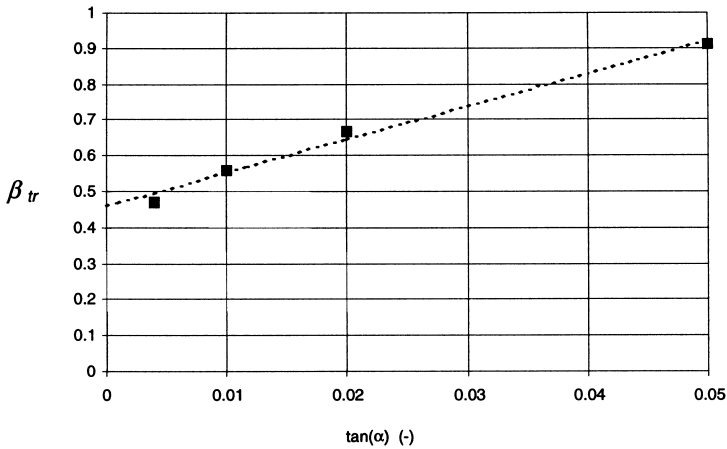


Fig. 6. Coefficients β_{tr} versus foreshore slope.

5.5. Root-mean square wave height

The fourth and last parameter to be estimated and parameterised is the rms wave height. Its estimation is trivial: we simply use the rms value of the sampled zero-crossing wave heights per record.

For a sequence of sine waves, the ratio $H_{rms}/\sqrt{m_0}$ equals $\sqrt{8} \approx 2.83$. It is well known that for nonlinear waves with narrow peaks and flat troughs (Stokes waves, cnoidal waves), this ratio is larger. Finite spectral bandwidth on the other hand tends to decrease this ratio. (For sea waves in deep water ($\psi \rightarrow 0$), with a broad banded frequency spectrum, $H_{rms}/\sqrt{m_0} \approx 2.69$, as mentioned above.) To investigate empirically the relation between H_{rms} and the total wave energy on shallow foreshores, where the waves are

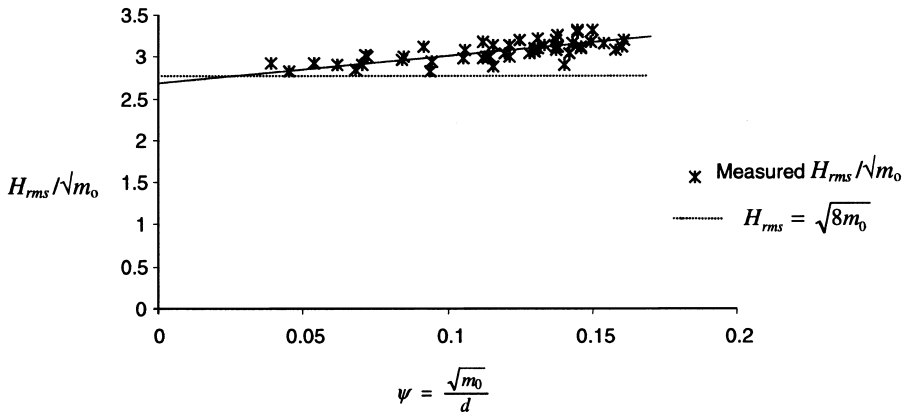


Fig. 7. Ratio $H_{rms}/\sqrt{m_0}$ measured on shallow foreshores versus the degree of saturation.

not sinusoidal and not necessarily narrow-banded, measured values of $H_{\text{rms}}/\sqrt{m_0}$ have been plotted versus the degree of saturation ψ for all slopes in Fig. 7. It is observed that in shallow water, the values of $H_{\text{rms}}/\sqrt{m_0}$ exceed the sine-wave value of $\sqrt{8}$, suggesting that here, the nonlinear effect outweighs that of the spectral bandwidth. (See Kuriyama, 1996 for an empirical parametric expression for a similar increase of the ratio $H_{1/3}/\sqrt{m_0}$ with increasing nonlinearity.) Using the deep-water ratio for broad-banded sea mentioned above (2.69) as a constraint, we assume

$$\frac{H_{\text{rms}}}{\sqrt{m_0}} = 2.69 + \beta_{\text{rms}} \psi \quad (11)$$

A least squares fit to the data in Fig. 7 yields $\beta_{\text{rms}} = 3.24$.

In the following, we refer to the CWD model with the above parameterisation of H_{rms} and with H_{tr} based on depth and bottom slope as point model (m_0, d, α) ; with H_{tr} based on wave period, water depth and bottom slope, we refer to point model $(m_0, d, \alpha, T_{0.2})$.

6. Validation of the model

The validation of the proposed point models is carried out by comparing predicted wave height distributions to the set of measured data selected for validation (Table 1). For comparison, this is also done for the Rayleigh distribution and the modified Glukhovskiy distribution.

An overall indicator of the approximation of the measured wave height distribution by a model is the relative rms error ε_{rms} , defined as:

$$\varepsilon_{\text{rms}} = \sqrt{\frac{1}{K} \sum_{k=1}^K \left(\frac{H_{N, \text{comp}}}{H_{N, \text{meas}}} - 1 \right)^2} \quad (12)$$

in which K denotes the number of records used and H_N denotes a wave height with probability of exceedance equal to N . Values of ε_{rms} have been determined for $H_{50\%}$, $H_{10\%}$, $H_{2\%}$, $H_{1\%}$, and $H_{0.1\%}$. Fig. 8 presents the results. Since the tests on shallow foreshores with slopes 1:30 and 1:50 were performed with 500 waves or less, no reliable $H_{0.1\%}$ is obtained for these. Therefore, no rms error for $H_{0.1\%}$ is presented in Fig. 8 for these slopes.

By averaging the rms errors of each model over the five selected wave heights, for a given slope, an overall insight in the approximation of measured wave height distributions by the three models is obtained. The results are shown in Fig. 9, for each slope separately. They show that the CWD point models yield the best approximation of the measured wave height distributions. The average reduction in rms error for both of them is about 60% compared to the conventional Rayleigh distribution and about 40% compared to the modified Glukhovskiy distribution (with $H_{\text{rms}} = \sqrt{8m_0}$ in both).

As stated before, the Miche-like transitional wave height parameterisation Eq. (9) has the disadvantage of a fourth input parameter $T_{0.2}$. Furthermore, Fig. 9 shows that the

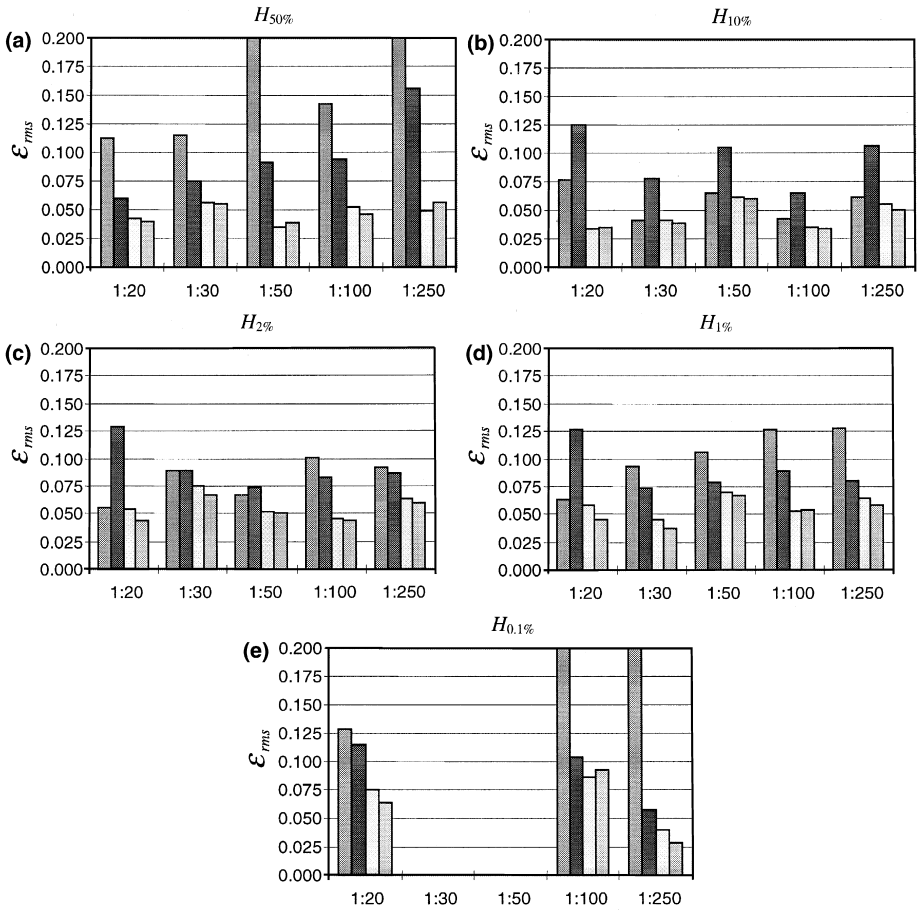


Fig. 8. Root-mean-square errors in characteristic wave heights for various foreshore slopes, for the Rayleigh, Glukhovskiy and the CWD point models (m_0, d, α) and ($m_0, d, \alpha, T_{0.2}$), respectively.

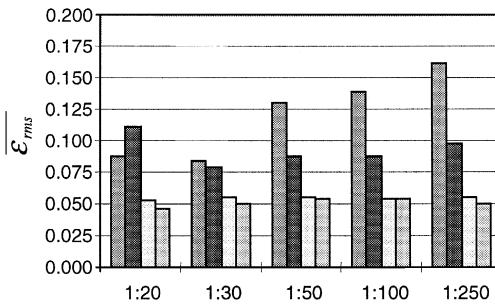


Fig. 9. Average root-mean-square error versus foreshore slope for the same models as in Fig. 8.

improvements obtained thereby are insignificant compared to those from the point model using a transitional wave height depending on the depth and bottom slope only, which does not require the definition and input information of a characteristic wave period. Therefore, the simpler parameterisation of the transitional wave height (Eq. (8)) is proposed, giving the point model (m_0, d, α) . Its properties are summarised below for easy reference in applications.

7. Summary of point model (m_0, d, α)

- cumulative distribution function: Eq. (5)
- continuity constraint: $F_1(H_{tr}) = F_2(H_{tr})$
- exponents: $k_1 = 2$ and $k_2 = 3.6$
- transitional wave height: $H_{tr} = (0.35 + 5.8 \tan \alpha)d$
- rms wave height: $H_{rms} = (2.69 + 3.24\sqrt{m_0/d})\sqrt{m_0}$
- normalised transitional wave height: $\tilde{H}_{tr} = H_{tr}/H_{rms}$

\tilde{H}_{tr} can be used to enter Table 2 in order to find desired statistical properties. If other properties are needed than those listed in Table 2, one should revert to the distribution function given in Eq. (5). The required (normalised) values of H_1 and H_2 can either be read from Table 2, if needed with some interpolation, or they can be calculated by solving the algebraic Eq. (7) together with the continuity constraint $(\tilde{H}_{tr}/\tilde{H}_1)^2 = (\tilde{H}_{tr}/\tilde{H}_2)^{3.6}$, for given values of k_1 , k_2 and \tilde{H}_{tr} .

7.1. Example

As an example of the application of the proposed point model (m_0, d, α) , and to illustrate its performance, we present here the calculation for the case shown in Fig. 1.

Calculate $H_{1/3}$, $H_{1\%}$ and $H_{0.1\%}$ at a location on a shallow foreshore with slope 1:100, still water depth $d = 0.27$ m, $m_0 = 1.1E - 3$ m² (so $\sqrt{m_0} = 0.033$ m and $\psi = \sqrt{m_0}/d = 0.123$).

1. $H_{tr} = (0.35 + 5.8 \tan \alpha)d = 0.408d = 0.110$ m
2. $H_{rms} = (2.69 + 3.24\sqrt{m_0/d})\sqrt{m_0} = 0.102$ m
3. $\tilde{H}_{tr} = H_{tr}/H_{rms} = 1.074$
4. Table 2 yields $\tilde{H}_{1/3} \approx 1.340$, $\tilde{H}_{1\%} \approx 1.697$ and $\tilde{H}_{0.1\%} \approx 1.900$
5. $H_{1/3} = \tilde{H}_{1/3}H_{rms} = 0.137$ m
6. $H_{1\%} = \tilde{H}_{1\%}H_{rms} = 0.174$ m
7. $H_{0.1\%} = \tilde{H}_{0.1\%}H_{rms} = 0.195$ m

The data points and the graph of the CWD for this case are shown in Fig. 10. The measured values of $H_{1\%}$ and $H_{0.1\%}$ can be read directly in this figure. The calculated values agree closely with these. Note that the results according to the classical Rayleigh distribution would be $H_{1/3} = 4\sqrt{m_0} = 0.132$ m, $H_{1\%} = \sqrt{(8 \ln 10^2)}\sqrt{m_0} = 0.200$ m and

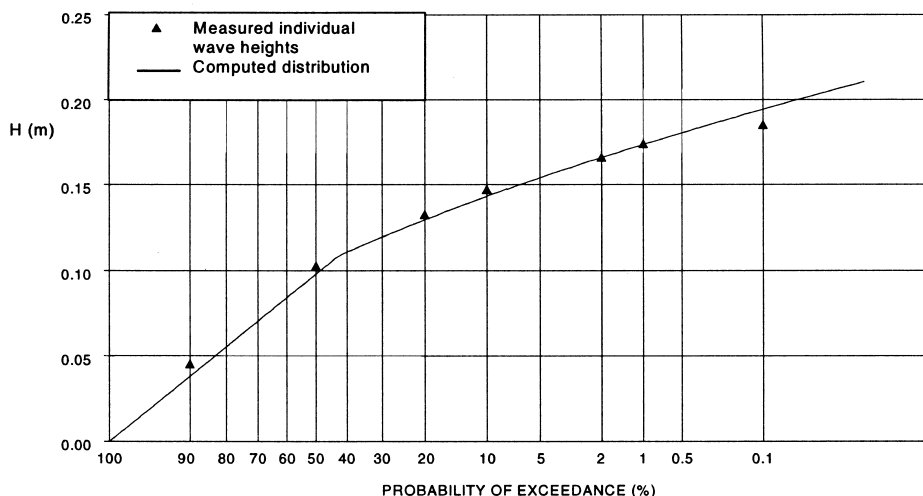


Fig. 10. Measured (solid triangles) and calculated (drawn line) wave height distribution on slope 1:100, $m_0 = 1.1E-3 \text{ m}^2$ and $d = 0.27 \text{ m}$.

$H_{0.1\%} = \sqrt{(8 \ln 10^3)} \sqrt{m_0} = 0.247 \text{ m}$ (see Fig. 1), or approximately 3% less, 15% more and 27% more than the values according to the proposed distribution and (approximately) the data.

8. Discussion

The material presented above indicates the variations that can occur in numerous relations that conventionally are considered as “universal”. This concerns ratios between characteristic wave heights on the one hand and between those and $\sqrt{m_0}$ on the other hand. It implies the need to be very specific in each case in the definitions of the quantities being considered.

The effect of wave breaking on the wave height distribution, for a given value of the local wave energy (given m_0), is to reduce the higher waves but at the same time to enhance the lower ones. However, nonlinearity of the wave profile tends to enhance the ratio of the wave heights to $\sqrt{m_0}$ (the leaner the waves, the higher they must be to carry the same potential energy), as can be seen for the rms wave height in Fig. 7. The effects cancel out to some extent for the intermediate wave heights, thus minimising the overall effect in such range. This is visible in the error plots in Fig. 8, which particularly for the Rayleigh distribution show the best performance in a range of intermediate wave heights, worsening both towards smaller and towards larger wave heights. The example given above also illustrates this: the Rayleigh distribution with $H_{\text{rms}} = \sqrt{(8m_0)}$ significantly overestimates wave heights with low exceedance probability (1% or 0.1%), whereas it makes only a relatively minor error (in fact a small underprediction) in estimating $H_{1/3}$.

Properties of the CWD are given in Table 2, for a range of the normalised transitional wave height from near-zero values to values sufficiently large for the Rayleigh distribution to be applicable for practical purposes. The minimal value that can actually be expected to occur is more restricted, however, because of the limited height-to-depth ratio. For a rough estimate of that minimum, we note that the degree of saturation ($\psi \equiv \sqrt{m_0}/d$) has a maximum (in our data) of about 0.16, which roughly corresponds to a maximum H_{rms} of about $0.5d$. The transitional wave height is of the same order (see Fig. 4), from which it follows that only the range of \tilde{H}_{tr} in excess of about 1 is realistic.

9. Conclusions

Waves on shallow foreshores are subject to depth-induced breaking, particularly the higher ones. This results in a profound change in the shape of the wave height distribution. A Composite Weibull distribution is proposed to describe the wave height distributions on shallow foreshores. Its parameters have been estimated and parameterised. This yields a model that predicts the local wave height distribution on shallow foreshores for a given local water depth, bottom slope and total wave energy with significantly greater accuracy than existing models.

List of symbols

Roman letters

A	coefficient in the Glukhovskiy distribution
d	still water depth
H	wave height
$H_{1/3}$	significant wave height; the mean of the highest 1/3-part of the wave heights
H_i	scale wave height of the CWD; $i = 1, 2$
H_{m_0}	spectral significant wave height, $H_{m_0} = 4\sqrt{m_0}$
H_N	wave height with exceedance probability $1/N$
H_{rms}	rms wave height
H_{tr}	transitional wave height of the CWD
\tilde{H}_x	normalised characteristic wave height, $\tilde{H}_x = H_x/H_{\text{rms}}$
H^*	ratio of rms wave height to water depth, H_{rms}/d
k_i	exponent in the CWD; $i = 1, 2$
L_c	characteristic wave length
L_{op}	deep water wave length based on peak period T_{op}
m_n	n th moment of the surface elevation frequency spectrum
m_0	variance of the surface elevation
$T_{0,2}$	wave period based on zero-th and second spectral moment, $T_{0,2} = \sqrt{m_0/m_2}$
T_c	characteristic wave period

Greek letters

α	slope of the foreshore
β	coefficient in the modified Glukhovskiy distribution

β_{rms}	empirical coefficient in the rms wave height parameterisation
β_{tr}	empirical coefficient in the transitional wave height parameterisation
ε_{rms}	rms error
γ_{tr}	empirical coefficient in the transitional wave height parameterisation
κ	exponent in the modified Glukhovskiy distribution
μ_H	mean wave height
ψ	degree of saturation, $\psi = \sqrt{m_0} / d$

Acknowledgements

The model was developed by the authors for mild slopes while HWG was a graduate student at the Delft University of Technology. It was extended to steeper slopes, including the parameterisation of the slope influence, while HWG was employed at WL/Delft Hydraulics. The interest and help of Dr. Marcel van Gent, WL/Delft Hydraulics, in making the data available and in useful discussions is gratefully acknowledged. The authors thank Martijn de Jong for numerical evaluations of the distribution function derived by Tayfun (1981). The constructive and helpful comments of the reviewers are gratefully acknowledged.

References

- Abramowitz, M., Stegun, I.A., 1964. In: Handbook of Mathematical Functions. Dover Publications, p. 260, 1046 pp.
- Bhageloe, G.S., 1998. Breakwaters with a single coverlayer (in Dutch), MSc Thesis Delft University of Technology; also Delft Hydraulics Report H3356, The Netherlands.
- Collins, J.I., 1970. Probabilities of breaking wave characteristics. Proc. 12th Int. Conf. Coastal Eng. I, 399–414.
- Dally, W.R., 1990. Random breaking waves: a closed-form solution for planar beaches. Coastal Eng. 14, 233–263.
- Dally, W.R., 1992. Random breaking waves: field verification of a wave-by-wave algorithm for engineering applications. Coastal Eng. 16, 369–397.
- Dally, W.R., Dean, R.G., 1986. Transformation of random breaking waves on surf beat. Proc. 20th Int. Conf. Coastal Eng. I, 109–123.
- Gerding, E., 1993. Toe stability of rubble mound breakwaters, Delft Hydraulics Report H1874, The Netherlands.
- Glukhovskiy, B.Kh., 1966. Investigation of sea wind waves (in Russian), Leningrad, Gidrometeo-izdat (reference obtained from E. Bouws (1979): Spectra of extreme wave conditions in the Southern North Sea considering the influence of water depth, Proc. of Sea Climatology Conference, Paris, pp. 51–71).
- Goda, Y., 1979. A review on statistical interpretation of wave data. In: Report of the Port and Harbour Research Institute, Japan 18 pp. 5–32.
- Groenendijk, H.W., 1998. Shallow foreshore wave height statistics, MSc Thesis, Department of Civil Engineering, Delft University of Technology.
- Groenendijk, H.W., van Gent, M.R.A., 1998. Shallow foreshore wave height statistics, Report H3351, WL/Delft hydraulics, The Netherlands.
- Klopman, G., 1996. Extreme wave heights in shallow water, Report H2486, WL/Delft hydraulics, The Netherlands.
- Kuriyama, Y., 1996. Models of wave height and fraction of breaking waves on a barred beach. Proc. 25th Int. Conf. Coastal Eng. I, 247–260.

- Longuet-Higgins, M.S., 1952. On the statistical distributions of heights of sea waves. *J. Mar. Res.* 11, 245–266.
- Longuet-Higgins, M.S., 1980. On the distribution of the heights of sea waves: some effects of nonlinearity and finite band width. *J. Geophys. Res.* 85, 1519–1523.
- Mase, H., Iwagaki, M., 1982. Wave height distributions and wave grouping in the surf zone. *Proc. 18th Int. Conf. Coastal Eng.*, 58–76.
- Miche, R., 1944. Mouvements ondulatoires de la mer en profondeur constante ou décroissante, *Annales des Ponts et Chaussées*, 114e Année, pp. 25–78, 131–164, 270–292, 369–406.
- Ochi, M.K., 1998. *Ocean Waves, the Stochastic Approach*. Cambridge Univ. Press, 319 pp.
- Tayfun, M.A., 1981. Breaking-limited wave heights, *ASCE. J. Waterway, Port, Coastal and Ocean Eng.* 107 (2), 59–69.
- Tayfun, M.A., 1990. Distribution of large wave heights, *ASCE. J. Waterway, Port, Coastal and Ocean Eng.* 116 (6), 686–707.
- Tayfun, M.A., 1999. Personal communication.
- Van der Meer, J.W., 1988. Wave heights of breaking waves on shallow slopes (in Dutch), Delft Hydraulics Report H0462.25, The Netherlands.